Subject: The All-Weather Wind Pod
Al Cooper
3 August 2014

Background

An all-weather wind pod has been developed by Allen Schanot and is available for mounting under the wing of the GV, where it was installed during the 2014 project DEEPWAVE. It uses a Rosemount 858 probe, but the location under the wing is one where there is substantial flow distortion in comparison to the free stream so an unconventional calibration is needed to use the measurements. The 858 probe is heated and should be unaffected by icing or ice accumulation, so this system has the potential to provide wind measurements in cases where icing or other problems cause failure of the standard radome-based system.

A preliminary calibration is in use now, but it does not appear to perform very well. The goal of this note is to develop a new calibration and demonstrate that the gust pod provides a valid alternative to wind measurements based on the radome.

The format of this note is that the text is interspersed with the R code that performed the processing. This file is located at cooperw/RStudio/DEEPWAVE/GustPodProcessor.Rnw and, if run from within the html interface to RStudio on tikal using the "Compile PDF" function, will produce this memo while processing a netCDF file to add new gust-probe variables to it. When this file is viewed in RStudio, grayed sections indicate R code. Some portions of that code are shown in this memo, but most are hidden; for the full code, see the above file.

A separate memo describes the calibration of the gust-pod measurements as well as those from the standard radome gust-sensing system; see "CalibrationPart1.pdf". The calibrations documented in that memo will be used in this processor, which adds gust-pod variables to a standard netCDF data file.

The Components of the Relative Wind

In the standard coordinate system with x forward, y starboard, and z downward, the three corresponding components of the relative wind are:

$$\mathbf{v} = \begin{pmatrix} u_r \\ v_r \\ w_r \end{pmatrix} = \begin{pmatrix} V \\ V \tan\beta \\ V \tan\alpha \end{pmatrix} \tag{1}$$

where V is the true airspeed, α is the angle of attack and β is the sideslip angle. The sign convention is such that the relative wind is positive when *from* the direction of the axis for each component.

Once the true airspeed V is known, (1) with appropriate values for angle of attack and sideslip will give the relative wind.

Transformation to an Earth Reference Frame

The gust-pod orientation is measured by an IRU in the pod, while the aircraft orientation is measured by a fuselage-mounted IRS. Each measures heading, pitch, and roll. There are again two alternate paths that can be followed: Transform to the aircraft reference frame and use the standard software (gusto.c), or transform to an Earth reference frame directly and use the gust-pod ground speeds to obtain the wind. The former takes advantage of the higher-quality IRU in the cabin, but involves additional complications arising from contributions of angular velocity of the aircraft and mis-alignment between the inertial systems. The latter course will be followed here, but it may be worth exploring if the former might give higher-quality measurements.

The required transformation is described by three rotation matrices, defined in Bulletin 23 Eqs. 2.5 and 2.6:

$$T_1 = \begin{pmatrix} 1 & 0 & 0 \\ 0 & \cos\phi & -\sin\phi \\ 0 & \sin\phi & \cos\phi \end{pmatrix}$$

$$T_2 = \begin{pmatrix} \cos\theta & 0 & \sin\theta \\ 0 & 1 & 0 \\ -\sin\theta & 0 & \cos\theta \end{pmatrix}$$

$$T_3 = \begin{pmatrix} \cos\psi & -\sin\psi & 0 \\ \sin\psi & \cos\psi & 0 \\ 0 & 0 & 1 \end{pmatrix}$$

where $\{\phi, \theta, \psi\}$ are {roll, pitch, heading}.

The transformation should be made in the following order:

1. Rotate by T_1 using the roll angle ϕ' measured by the gust-pod IRU (CROLL_GP) to level the wings by a rotation about the x axis.

2. Rotate by T_2 using the pitch angle θ' (CPITCH_GP) to level the aircraft by a rotation about the y axis.

3. Rotate by T_3 using the heading angle ψ' (CTHDG_GP) to obtain components in a true-north reference frame. At this point, the relative-wind vector in an Earth-reference coordinate system is $\mathbf{v}_r = T_3(T_2(T_1\mathbf{v}))$ where $\mathbf{v}$ is given by (1).

At this point, the measured ground-speeds of the gust pod can be added to the relative wind to get the true Earth-relative wind.

The transformations coded here are described by the matrices T_1, T_2, and T_3 defined above. Although the following is coded as a 'for' loop, full matrices are calculated here that represent

the sample-by-sample transformations in anticipation that a vector implementation of this can be found. That is the reason than data-array-length vectors containing 1 or 0 are defined as well as vectors cosphi, ..., representing the trigonometric functions of the attitude angles.

The relative-wind vector in an Earth-reference coordinate system is $\mathbf{v}_r = T_3(T_2(T_1\mathbf{v}))$ where $\mathbf{v}$ is given by (1). Next, the measured ground-speeds of the gust pod can be added to the relative wind to get the true Earth-relative wind. The final equations. defining new wind variables {WDG, WSG, WIG} corresponding to {WDC, WSC, WIC} from the radome gust system, are:

$$\mathbf{v}_g = \mathbf{v}_r + \begin{pmatrix} -\text{CVNS\_GP} \\ -\text{CVEW\_GP} \\ \text{CVSPD\_GP} \end{pmatrix} \tag{2}$$

$$\text{WDG} = \arctan 2(v_{g,y},\ v_{g,x}) \tag{3}$$

$$\text{WSG} = \sqrt{(v_{g,x}^2 + v_{g,y}^2)} \tag{4}$$

$$\text{WIG} = v_{g,z} \tag{5}$$

To be comparable to {WDC, WSC, WIC}, however, the same complementary filter should be applied that adjusts VEW and VNS by comparison to GGVEW and GGVNS. This is accomplished by running the same complementary filter on CVEW_GP and CVNS_GP as used for VEW and VNS, before using them as above to find the wind components.

The code also attempts to flag bad CTHDG_GP measurements, which apparently occur as the heading moves through 180 deg. This would be better replaced by interpolation at these points.

Here are some plots that show the results. For similar results from DEEPWAVE rf05, saved for reference, see GPcal.pdf, a note saved on 22 June 2014.

```
## [1] "Flight processed in this run: " "rf16"
## [1] "File Times: "        "2014-07-04 04:24:11" " to "
## [4] "2014-07-04 13:13:54"
```

```
## [1] -0.4218
## [1] 0.5285
```

```
## NULL
## NULL
```

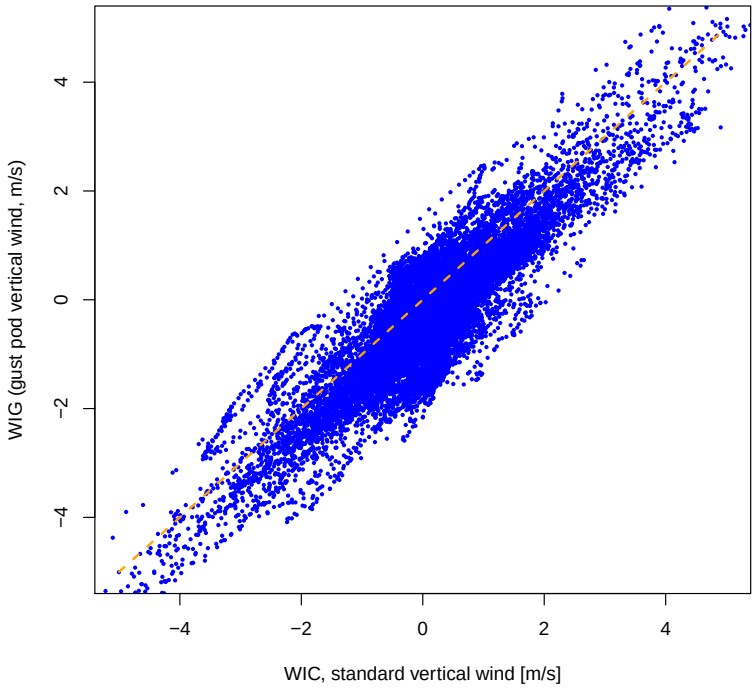

Figure 1: WIG (vertical wind based on the gust pod) plotted against WIC (vertical wind from the conventional radome-based gust system)

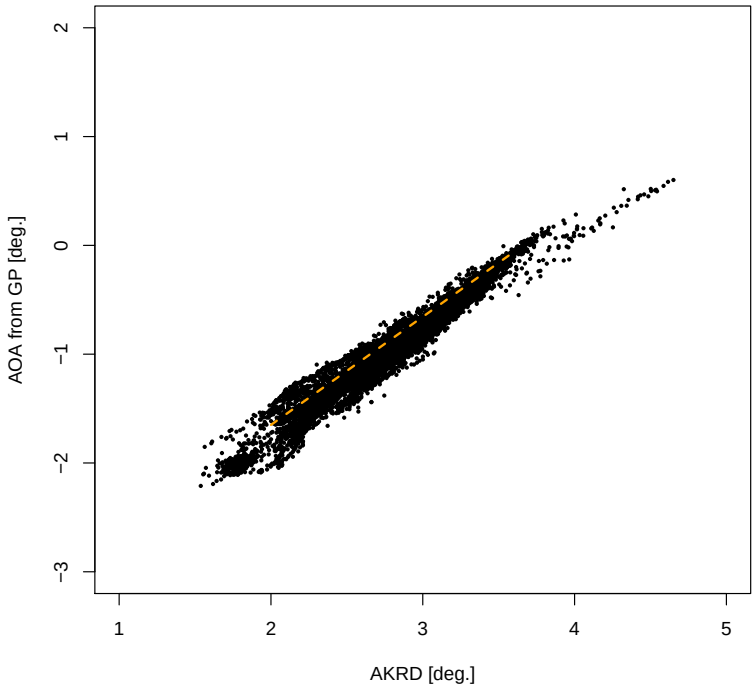

Figure 2: Angle of attack determined from gust-pod measurements, plotted vs. corresponding measurements AKRD from the standard wind sensing system

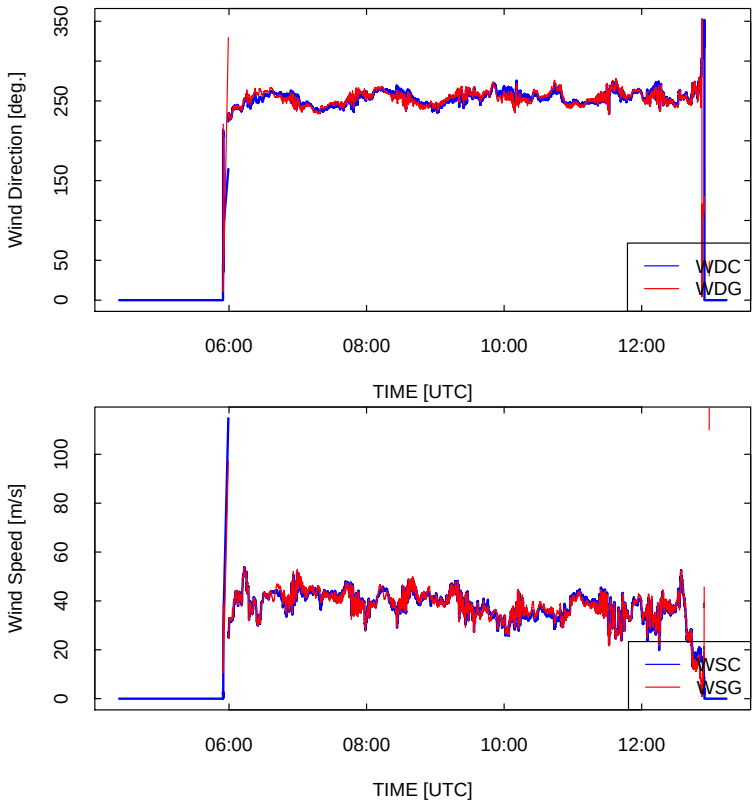

Figure 3: Comparison of horizontal wind measurements from the gust pod (red lines) and from the standard wind measurements WDC and WSC (thicker blue lines).

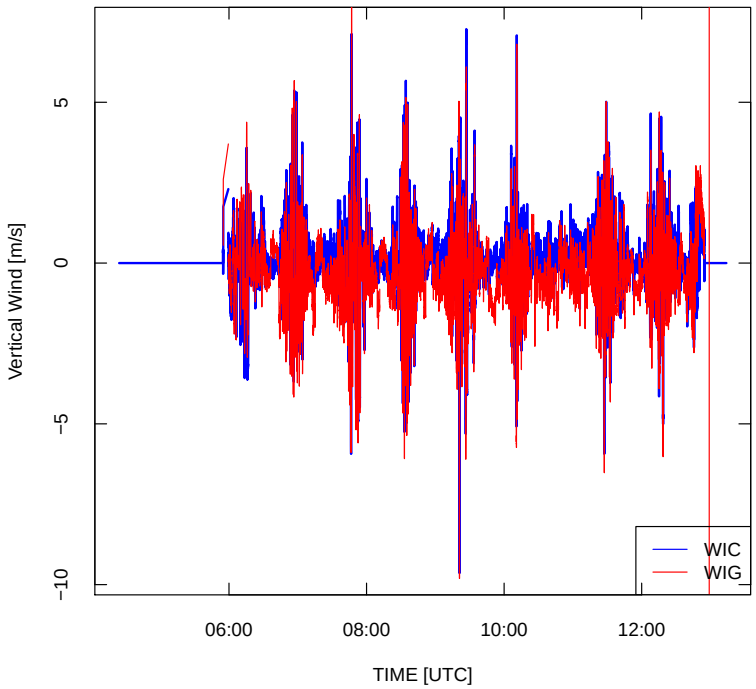

Figure 4: Comparison of vertical wind measurements from the gust pod (red line) and from the standard wind measurement (WIC, blue line).

```
## NULL
```

Mixing of Attitude Angles for the Gust Pod

One problem that arises with the gust pod is that the orientation is such that the attitude angles (pitch, roll, heading) are defined relative to the orientation of the inertial unit in the gust pod, which is not aligned with the longitudinal axis of the aircraft. As a result, the roll introduced in turns, even if primarily a rotation about the aircraft longitudinal axis, will appear as a combination of attitude-angle changes in the gust pod. Errors arising from the initial alignment at the start of flights will also cause problems with the measured attitude angles, and it is likely that these will be more significant near the start of flights because the build-in Kalman filter will us GPS measurements to correct such errors in the course of the flight.

This problem with the reference frame for attitude angles will have two consequences:

1. Measurements from the gust pod in turns will likely have large errors in comparison to the errors in level flight. The measurements from the gust pod should probably be flagged as of

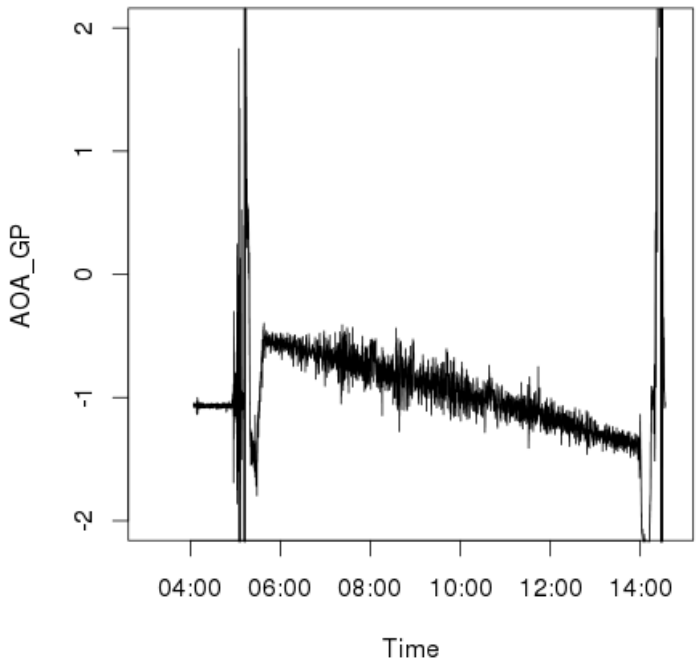

Figure 5: Angle of attack measured by the gust-pod system on DEEPWAVE flight RF18.

poor quality whenever the roll exceeds some threshold like perhaps $\pm 5^\circ$. (The measurements often look reasonable in turns despite this worry.)

2. There may be an offset introduced by the mixing of sideslip and angle-of-attack, and this will affect the reference or average value of the measured vertical wind, sometimes introducing a significant offset.

Because the weight of the aircraft decreases during the flight, so does the angle-of-attack, as shown in Fig. 5. Because the wing flexes, the measured sideslip also varies with time, as shown by Fig. 6, so there will be an offset in sideslip that will affect the mean lateral component of the wind. In addition, this flight had a particularly large offset in the vertical wind from the gust pod (WIG) at the start of the flight, as shown in Fig. 7. This offset is associated with a brief period where the difference in heading between the IRU in the gust pod and that in the fuselage were unusually large, as shown in Fig. 8. In addition, the mean value of the measured roll was close to zero for the in-cabin IRU but about 1.375° for the gust-pod IRU. Coupling among these attitude angles appears to have caused the large offset in WIG at the start of this flight. Because the gust-pod IRU incorporates a Kalman filter that can use measured errors in position and ground speed as determined by comparison to a GPS measurement to refine the measurements, the large error appears to have been corrected as the flight progressed.

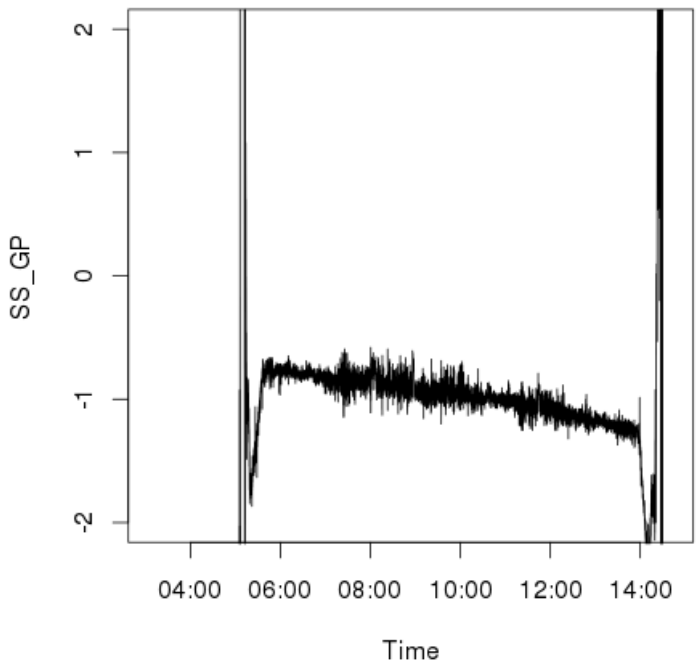

Figure 6: Sideslip angle measured by the gust-pod system on DEEPWAVE flight RF18.

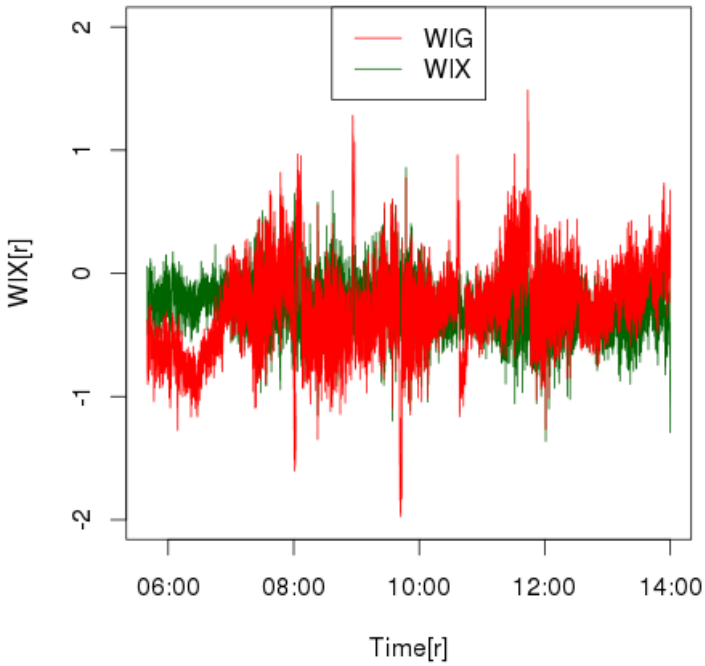

Figure 7: The vertical wind determined by the gust pod (WIG) and via standard processing (WIX, to distinguish this from WIC as determined by erronous in-field processing), for flight RF18 of the DEEPWAVE project.

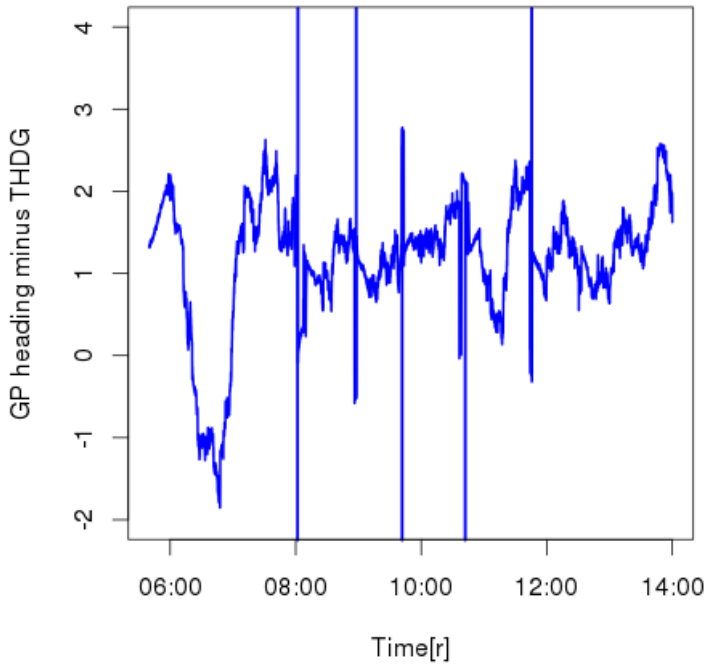

Figure 8: The difference in heading between the values measured by the IRU in the gust pod and the IRU in the cabin, for DEEPWAVE flight RF18.

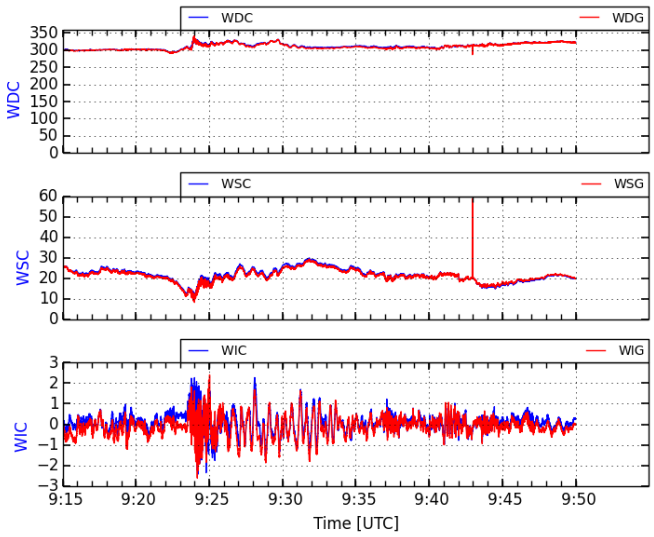

Figure 9: A comparison between the conventional wind components (blue lines) and the wind from the gust pod (red lines). Data from flight RF05.

These effects suggest that the vertical wind measured by the gust pod may have an offset in some cases, particularly at the start of flights, and the sideslip can also have an offset that will contribute to the lateral component of the measured wind. These are weaknesses in the measurements from the gust pod that, at this stage, do not appear easily corrected. A future study implementing Schuler tuning in a post-processing step and correcting for the entwined-angle effects may be able to reduce these weaknesses, but that will require a more extensive research project than possible prior to processing of DEEPWAVE data.

Additional Illustrative Plots

Some plots showing the nature of the new variables (WDG, WSG, WIG) are included here. The first one (Fig. 9) shows a comparison of all three wind variables for a segment from flight RF11. The spike in WSG at about 9:43 has a known origin and will be removed. There is also a short period near 9:23 when the vertical wind measurements appear offset by a few tenths m/s. Otherwise, the gust pod provides a good representation of the standard variables. Figure 10 shows an expanded view and emphasizes the small difference between wind speeds from the two systems; this is likely caused by IRU differences and can later be improved by reference to the GPS signals with OMNISTAR. The similarities and differences in WIG vs WIC are also more evident in this figure.

Figure 11 shows the high-rate variance spectra from the two systems. There is a significant difference at frequencies above about 3 Hz, with the gust-pod distribution dropping faster but the standard wind WIC showing more variance. The high frequency spectrum from the gust pod may

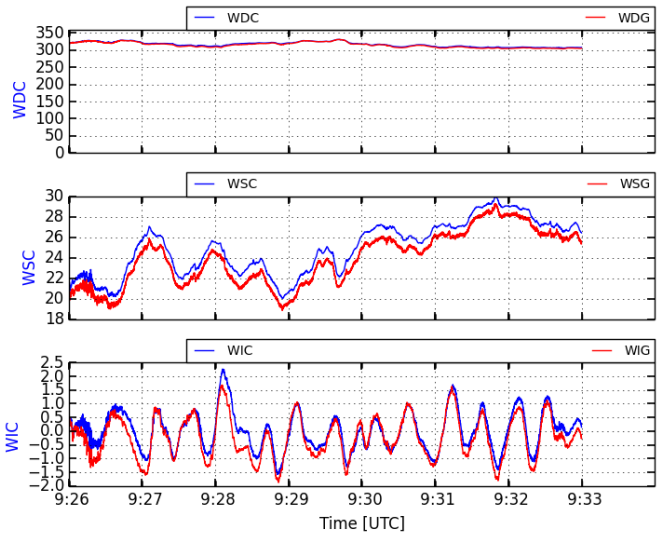

Figure 10: An expanded view of a section of Fig. 9.

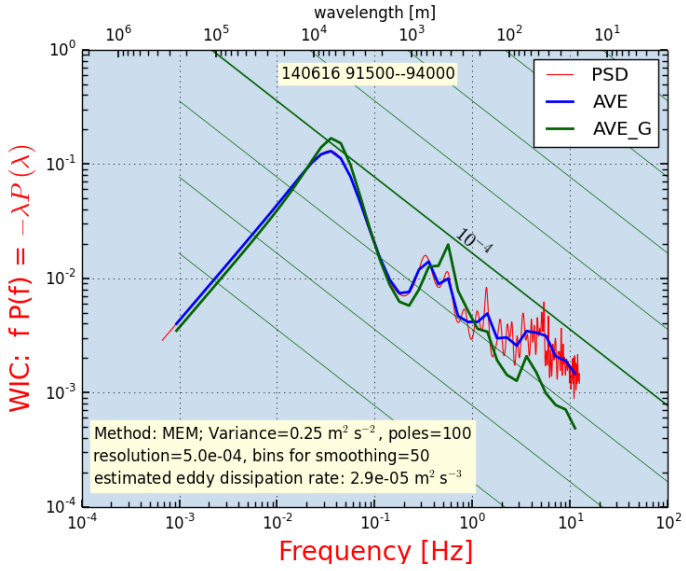

Figure 11: variance spectra for WIC (red line, and also shown smoothed as the blue line), compared to the spectrum for WIG from the gust pod (green line). Data from flight RF05, 9:15:00–9:40:00.

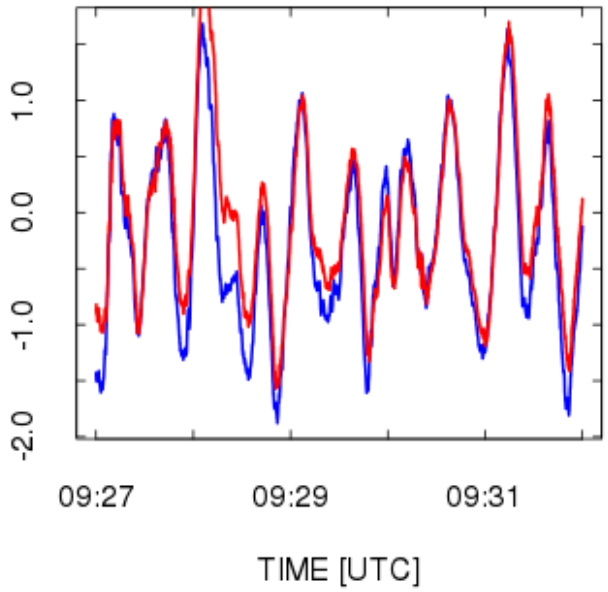

Figure 12: Comparison of WIG (red line) and WIC (blue line) after shifting WIG 1/25 s earlier to compensate for the longitudinal displacement of the sensor.

be more realistic; it is unusual to see high variance at these frequencies without a related generating source. These spectra were also studied for coherence, which was above 0.9 for frequencies less than 1 Hz but then fell to around 0.2 at 10 Hz. This is an indication that the two measurements are different in important ways at the high frequency. This would not be the case if they were responding with different amplitudes; the signals must really be mostly incoherent at the highest frequency. The separation wing-to-fuselage is about 7 m lateral and 13 m longitudinal, so that doesn't seem enough to cause the low high-frequency coherence. The phase changes from in-phase at frequencies less than 1 Hz to 180° out-of-phase at 9 Hz, with WIG lagging, so this is consistent with the longitudinal offset. Shifting WIG relative to WIC also gave maximum coherence if WIG were shifted forward 1/25 s. With this shift, there does not appear to be any difference in phase between the two measurements.

It is important to note that the gust pod does not yet perform well in turns. The reason is that the orientation of the gust-pod IRU is not perfectly along the longitudinal axis of the aircraft, and as a result any roll of the aircraft introduces complex combinations of roll, heading, and pitch into the gust-pod IRU. It should be possible to remove these to some extent, although differences in alignment of the IRU from flight to flight may perturb these angles and make it difficult to get good measurements in turns. The circle maneuvers from the calibration flight should provide valuable information regarding the potential for improving the in-turn performance of the gust pod

.

Next Steps

1. A procedure for processing the gust-pod measurements will be needed. It may be possible to use code in gusto.c for this purpose or otherwise to implement the process used here into nimbus, because this is being done second-by-second as needed for nimbus. Alternately, the code used here can run after nimbus processing to add the gust-pod variables. If this course is followed, the R script could be improved because I didn't vectorize the angle transformations yet, in the interest of getting it to work first. The software / data processing group will have to decide which is better, and it may be preferable to use different procedures for DEEPWAVE and for future use in order to produce the DEEPWAVE data quickly.

2. As noted above, there are issues with the gust-pod measurements in turns that need to be addressed. These issues will affect the standard data also because in turbulence the roll changes and this may feed into the other measurements even at small roll angles.

3. The relative timing of the measurements entering the calculation of wind still needs to be addressed. The IRU information is transmitted for recording with some delay, and corrections for those delays are in place. However, small errors in those delays can cause phase shifts among the measurements that, for example, result in residual perturbations of the vertical wind during pitch maneuvers. These should be tuned to minimize those perturbations.

4. An additional worthwhile study will be to see if using GPS measurements to determine the Schuler oscillation can improve measurements of pitch and heading and so lead to improved wind measurements. There is some evidence of this problem in an apparent changing offset in the vertical wind, so any improvement here can be very useful to DEEPWAVE.

– End of This Note –